Supplement of Earth Surf. Dynam., 9, 333–350, 2021
https://doi.org/10.5194/esurf-9-333-2021-supplement

Supplement of

Effect of stress history on sediment transport and channel adjustment in graded gravel-bed rivers

Chenge An et al.

Correspondence to: Xudong Fu (xdfu@tsinghua.edu.cn)

S1. DEM of bed surface during the experiment

This section shows the DEM of bed surface at different time during the experiment. Results of REF6 (15) which has the longest duration of conditioning phase is presented here as an example, as shown in Fig. S1. Direct observation shows that major channel deformation (degradation) occurs during the conditioning phase and Step 4 of the hydrograph phase, which is in agreement with our results presented in Section 3.1 (Fig. 3) of the main text.

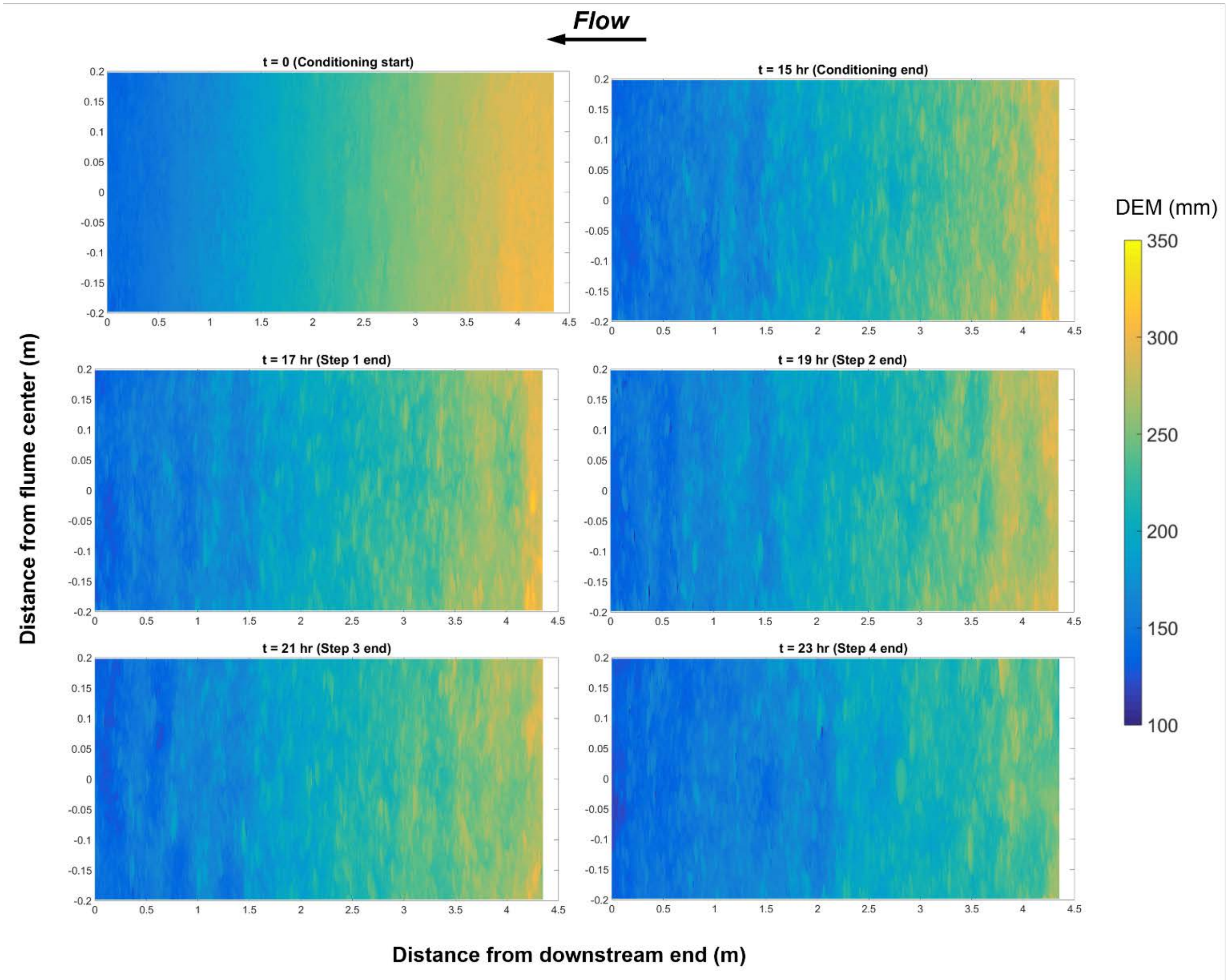

Figure S1. DEM of bed surface at different times during the experiment of REF6 (15), which has the longest duration of conditioning phase.

S2. Uncertaity analysis of light table measurement

Dynamics of sediment transport measured by the light table is presented and analyzed in the main text, in terms of both total transport rate and characteristic grain sizes. In this section, we provide detailed estimation of the uncertainty of light table measurement by comparing the light table data against the sediment trap data for all experiments. Fig. S2(a) shows the uncertainties associated with the total sediment transport rate. It can be seen that the light table data and the sediment trap data show good agreement. The light table overestimates the total sediment transport rates by 4% on average (111 samples and a standard deviation of 14.5%). 70 out of 111 samples show an accuracy of ±10% and 93 out of 111 samples show an accuracy of ±20%.

Uncertainties associated with the bedload characteristic grain sizes are presented in Fig. S2(b). The D_{50} of bedload measured by light table show relatively good agreement with that measured by trap. The light table overestimates the D_{l50} by only 3% on average (111 samples and a standard deviation of 40.1%). 91 out of 111 samples show an accuracy of ±50% for D_{l50}. Accuracy of D_{l10} and D_{l90} is not as good as that of D_{l50}. The light table underestimates the D_{l10} by 20% on average (111 samples and a standard deviation of 39.0%), and overestimates the D_{l90} by 30% on average (111 samples and a standard deviation of 26.5%). 71 out of 111 samples show an accuracy of ±50% for D_{l10} and 91 out of 111 samples show an accuracy of ±50% for D_{l90}.

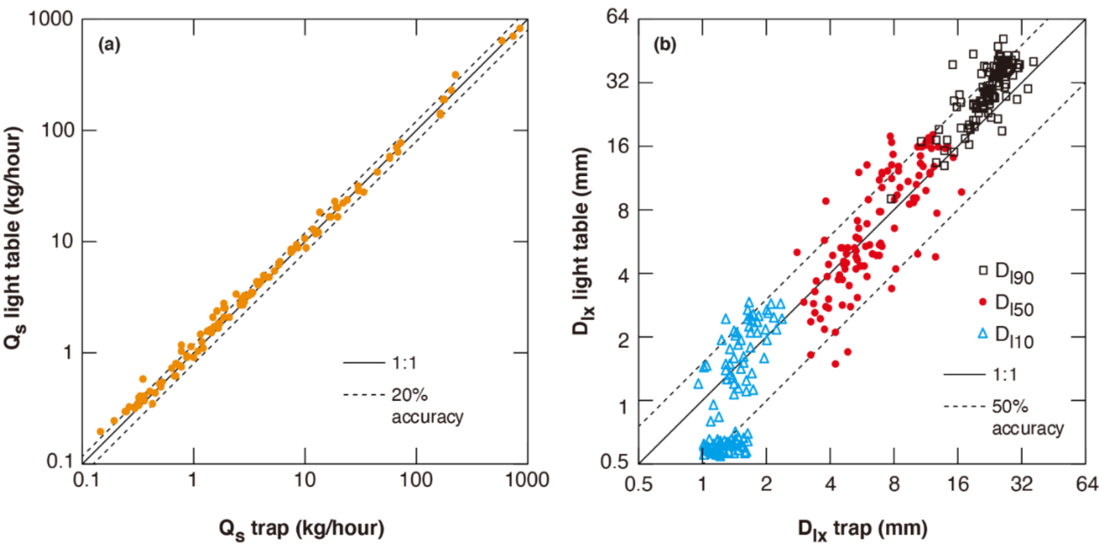

Figure S2. Comparison between the light table data and the sediment trap data for all experiments. (a) Total sediment transport rate; (b) D_{10}, D_{50}, and D_{90} of the bedload.

S3. Regression of sediment transport rates against the exponential function

In this section, we fit the instantaneous sediment transport rates during the conditioning phase of our experiment by a two-parameter exponential function. Previous researchers (Haynes and Pender, 2007; Masteller and Finnegan, 2017) have suggested that the exponential function can be implemented to describe the temporal decrease of sediment transport rate under conditioning flow. Here two of our experiments with the longest duration of conditioning phase (REF2 (15) and REF6 (15)) are analyzed. Results are shown in Fig. S3. As we can see from the figure, the fitted exponential function can describe the general decreasing trend of sediment transport rate during the conditioning phase, except at the beginning of the conditioning phase where the decrease of sediment transport rate is much more significant than predicted by the exponential function. Moreover, for the two experiments, the exponential function shows very similar values of regression parameters.

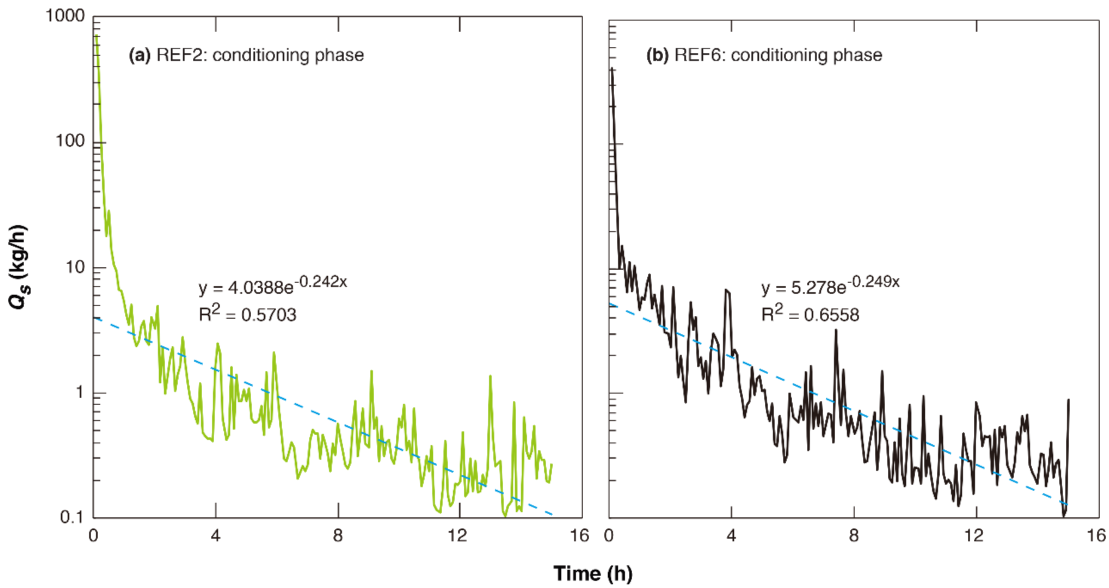

Figure S3. Regression of sediment transport rates during the conditioning phase, using an exponential function. (a) REF2 (15); (b) REF6 (15). Solid lines denote instantaneous sediment transport rates measured by light table. Dash lines denote calibrated exponential functions. The regression parameters and correlation coefficient are also shown in the figure.

S4. Sediment mobility of each size range during the experiment

In this section, we analyze the sediment mobility of each size range during the experiments. Figure S4 shows the scaled fractional sediment transport rate $Q_s p_i/F_i$ at different time of the experiment based on the light table data, where p_i denotes the volume fraction of the i-th size range in the bedload and F_i denotes the volume fraction of the i-th size range on the bed surface. By scaling on the bed surface fraction, the scaled fractional sediment transport rate thus represents the mobility of each size range: the larger the scaled fractional sediment transport rate is, the larger is the sediment mobility of this size range. In Fig. S4(a), the sediment mobility of different experiment is similar and each experiment shows an approximately horizontal line with the grain size, indicating that equal mobility (i.e., the GSD of sediment load matches the GSD of sediment on bed surface) dominates at the beginning of the conditioning phase. At the end of the conditioning phase (as shown in Fig. S4(b)), the mobility among experiments becomes different: the shorter the duration of the conditioning phase, the larger is the overall mobility. Moreover, the experiment with the shortest conditioning duration (i.e., REF7 (0.25)) is still near equal mobility, except that the mobility of the finest size range is larger than other size ranges. Whereas other experiments have become partial mobility with evident selective transport for sediment finer than 16 mm and almost no mobility for sediment coarser than 16 mm. This agrees with the observation by Ockelford et al. (2019) that bedload transport is characterized by equal mobility with no conditioning flow, but becomes more strongly size selective in the coarse and fine end members of the distribution as the duration of conditioning flow increases. Two isolated dots are observed at the very coarse end in REF5 (5) and REF6 (15) due to sampling inaccuracy of the light table. At the end of Step 1 and Step 2, all experiments show evident selective transport or partial mobility, as shown in Figs. S4(c) and S4(d). With the increase of flow discharge and sediment supply, the sediment transport regime in all experiments gradually return to equal mobility with coarse particles being mobilized at the end of Step 3 and Step 4. The difference of mobility among experiments during hydrograph is smaller compared with that at the end of the conditioning phase, and also becomes no longer correlated with the duration of conditioning flow.

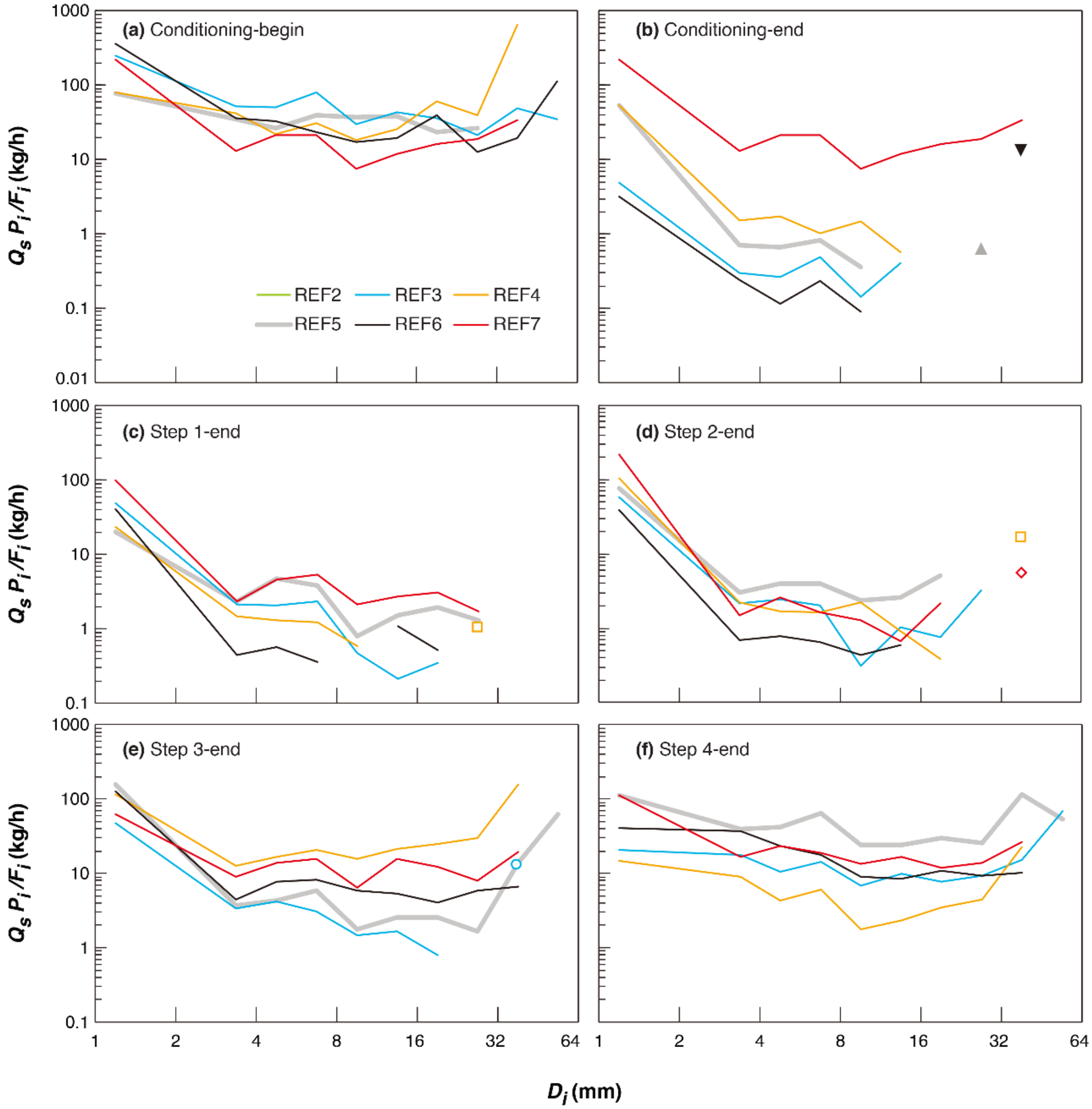

Figure S4. Scaled fractional sediment transport rate at different time of the experiment: (a) start of the conditioning phase (t = 15 mins); (b) end of the conditioning phase; (c) end of Step 1 of the hydrograph; (d) end of Step 2 of the hydrograph; (e) end of Step 3 of the hydrograph; (f) end of Step 4 of the hydrograph.

References

Haynes, H., and Pender, G.: Stress history effects on graded bed stability, Journal of Hydraulic Engineering, 33, 343–349, 2007.

Masteller, C. C., and Finnegan, N. J.: Interplay between grain protrusion and sediment entrainment in an experimental flume, Journal of Geophysical Research-Earth Surface, 122, 274–289, https://doi.org/10.1002/2017GL076747, 2017.

Ockelford, A., Woodcock, S., and Haynes, H.: The impart of inter-flood duration on non-cohesive sediment bed stability, Earth Surface Processes and Landforms, 44, 2861-2871, doi:10.1002/esp.4713, 2019.